Transactions of the Materials Research Society of Japan 29 [8] 3507-3510 (2004)

Misorientation change during annealing of Al heavily deformed by accumulative roll-bonding (ARB)

X. Huang, R. Ueji*, N. Tsuji* and N. Hansen
Center for Fundamental Research: Metal Structures in Four Dimensions, Materials Research Department, Risø National Laboratory, DK-4000 Roskilde, Denmark
Fax: 45-4677-5758, e-mail: xiaoxu.huang@risoe.dk
*Department of Adaptive Machine Systems, Osaka University, 2-1 Yamadaoka, Suita, Osaka 565-0871, Japan
Fax: 81-6-6879-7434, e-mail: tsuji@ams.eng.osaka-u.ac.jp

Commercial purity aluminum has been deformed by accumulative roll bonding (ARB) up to a strain of 4.8, followed by annealing for 30 min at temperatures 150 and 300°C, respectively. The microstructure and the misorientation characteristics (including the fraction of high angle boundaries (>15°) and the misorientation distribution) have been examined for the as-deformed state and for the annealed samples. A lamellar structure characterizes the microstructure in the as-deformed state and the low temperature annealing, while an equiaxed structure is formed when the sample is annealed at 300°C. The fraction of high angle boundaries was measured to be as high as 56% in the deformed sample, and this fraction showed a slight increase with increasing annealing temperature as a result of a decrease in the fraction of low angle boundaries.

Key words: ARB, aluminum, misorientation, transmission electron microscopy, annealing.

1. INTRODUCTION

Accumulative roll-bonding (ARB) process can impose very high plastic strains into various metals and alloys, and consequently result in a significant refinement in structure and an increase in strength [1-5]. Another important effect of the high strains is on the annealing behavior of the deformed samples where the microstructural change during annealing may differ from that well established for low to medium strain samples. In this study, a commercial purity Al has been deformed by ARB to a nominal strain of 4.8 and the microstructural changes during annealing at different temperatures are followed by transmission electron microscopy (TEM) and electron backscatter diffraction (EBSD). Particular attention is paid to the evolution in the boundary misorientation angle which is a key parameter in characterizing the annealing behavior of high strain structures.

2. EXPERIMENTAL PROCEDURES

Commercial purity aluminum sheets (1100, 99.1%Al, $1mm^t$ x $40mm^w$ x $300mm^l$) were used in this study. The initial microstructure was a fully recrystallized grain structure with a mean grain size of 18μm. The sheets were deformed by ARB to 6 cycles. The roll-bonding was performed at room temperature by use of a two-high mill with a roll diameter of 310mm at a roll peripheral speed of 17.5 $m \cdot min^{-1}$. The surface of the roll was kept in dry condition without any lubricant. Reduction in thickness per ARB cycle was 50% (corresponding to an equivalent von Mises strain 0.8), and it was applied in one rolling pass. The total equivalent strain is therefore 4.8 after 6 cycles. The deformed specimens were subsequently annealed for 1.8ks at 150°C, and 300°C, respectively.

The as-deformed and the annealed specimens were examined by transmission electron microscopy (TEM) and electron backscatter diffraction (EBSD) in a field emission gun scanning electron microscope. All examinations by TEM and EBSD were carried out in the longitudinal plane containing the normal and rolling directions (ND and RD). A semiautomatic Kikuchi line method was used for measurement of crystallographic orientations in TEM [7]. EBSD analysis was performed using TSL software.

3. RESULTS

3.1 Microstructure and misorientation in the as-deformed state

The deformation microstructure after 6 ARB cycles has been characterized previously [6], showing a well-developed lamellar structure, as shown in Figure1a. The lamellar structure is delineated by extended lamellar boundaries parallel to the rolling plane. Short dislocation boundaries interconnecting the lamellar boundaries are also formed between the lamellar boundaries. The mean spacing of the lamellar boundaries is 0.20μm, and the mean spacing of interconnecting boundaries is 0.57μm. The aspect ratio is 2.9. To characterize the spatial distribution of misorientations, the misorientation angles across the lamellar boundaries and the interconnecting boundaries were measured in TEM. Figure 1b shows an example of misorientation mapping, and the analyzed area is indicated in figure 1a by a white rectangle. In this map, high-angle boundaries with misorientation angles larger than 15° are drawn by bold lines, while low angle boundaries with misorientation angles smaller than 15° are drawn by thin lines. The dashed lines are the boundaries whose misorientations were not measured.

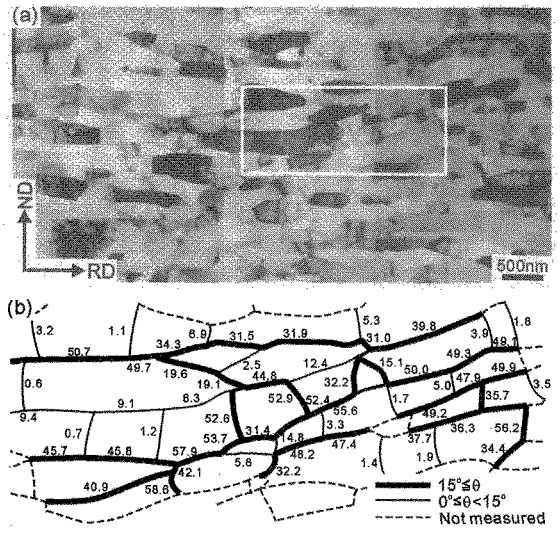

Figure 1 (a) Transmission electron micrograph showing the microstructure of aluminum deformed by ARB to 6 cycles and (b) the corresponding illustration of misorientation mapping.

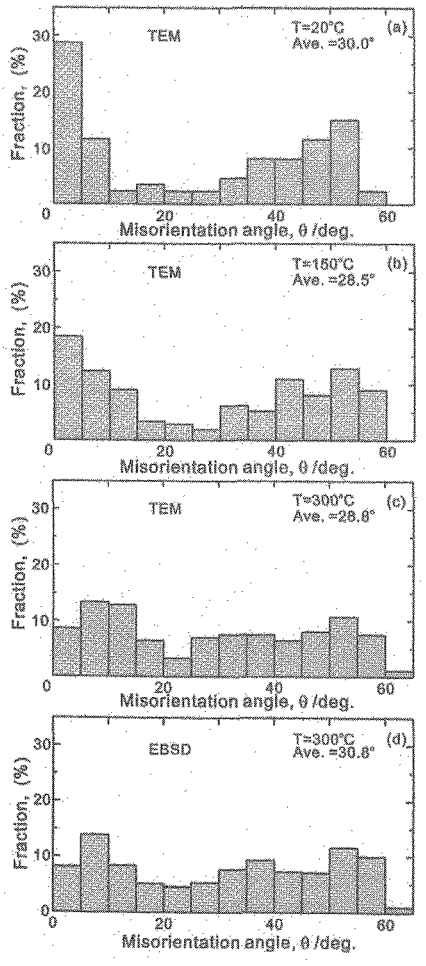

Figure2. Distributions of boundary misorientation angles before and after annealing at different temperatures.

Almost all of the lamellar boundaries are high-angle boundaries, whereas the short interconnecting boundaries have a mixture of low and high angles. The misorientation distribution in the deformed state is shown in figure 2a. The mean misorientation angle is 30.0° and the fraction of high angle boundaries in the microstructure is 56%. To be noted is that some of the interconnecting boundaries have rather small misorientation angles (see figure 1a), and an analysis of the misorientation distribution gives that there is 17.2% of the total boundaries having misorientation angles below 2.5°.

3.2. Microstructure and misorientation in the annealed samples

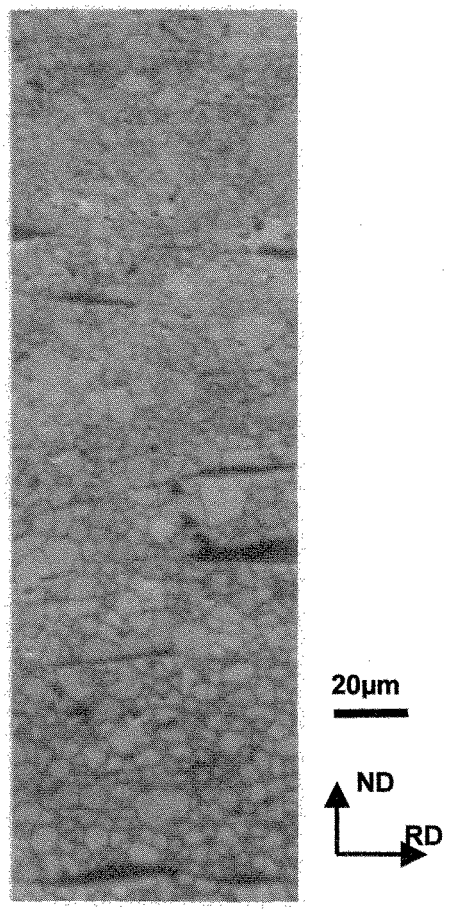

Figure 3. An EBSD IQ image showing the equiaxed structure after an annealing for 30min at 300°C.

After an annealing for 30min at 150°C, the morphology shows still a lamellar structure with a lamellar boundary spacing 0.3 μm that is slightly larger than the value (0.2 μm) obtained in the as-deformed sample. However, the TEM observations and the EBSD images showed the formation of an equiaxed structure after an annealing at 300°C. The boundary spacing was measured to be 4.6 μm and the dislocation density within the (sub)grains is rather low. Such an equiaxed

structural feature is illustrated in the IQ map of an EBSD image covering a relatively large area. The structure is relatively uniform, although an existence of grains with relatively larger sizes may be seen. The elongated black traces (low pattern quality areas) seen in figure 3 correspond to the bounded interfaces where a very fine structure mixed with a small amount of oxides did not allow a proper indexing of the EBSD patterns in these areas. It is interesting to note that some of the grains of large sizes have flat interfaces with the bonded interfaces. This indicates that the bonded layers have a pinning effect on the grain growth, probably due to the oxides dispersed during the wire brushing and the roll-bonding.

Figures 2b and 2c show the distributions of misorientation angles measured by TEM in the samples annealed at 150°C and 300°C, respectively. It is seen that the fraction of boundaries with misorientation angles less than 15° decreases and that with misorientation angles in the range 15-40° increases with increasing annealing temperature. An analysis of the TEM results for the 300°C annealing (figure 2c) shows that there is only 5.3% of the measured boundaries having misorientation angles smaller than 2.5°. Therefore, a cut off angle of 2.5° is used for plotting the distribution of misorientation angles measured for the same sample by EBSD, and the result is shown in Figure 2d. Note that the distribution in figure 2d is obtained based on a measurement over a rather large area (see figure 3). A comparison between figures 2c and 2d shows a good agreement between the TEM and EBSD results: the fractions of high angle boundaries are 65.2% and 69.4%, respectively, in the two cases.

Figure 4 shows the fraction of high angle boundaries as a function of annealing temperature. A slight increase with temperature is seen, which corresponds to the decrease in the fraction of low angle boundaries as seen in Figures 2a-c.

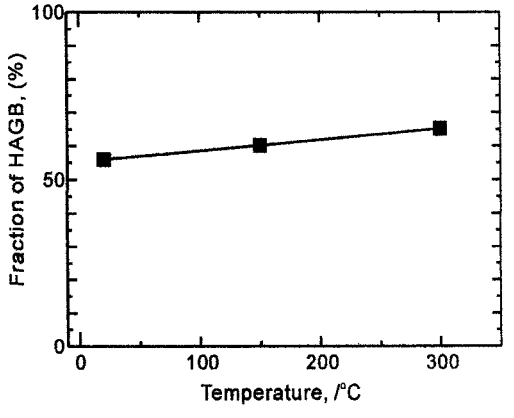

Figure 4. The fraction of high angle boundaries in the as-deformed sample and in the samples annealed at 150°C and 300°C, respectively.

4. DISCUSSIONS

4.1 Misorientation evolution

The TEM results of misorientation measurements show that a large fraction, 56%, of high angle boundaries is developed in the as-deformed sample (Figure 2a), which is a rather high percentage compared with that (about 35%) obtained in a commercial purity of aluminum deformed by conventional cold-rolling to a similar strain [8]. This observation has been discussed in [9], and the higher misorientation angles has been attributed to the additional contribution of the redundant shear strain involved in the ARB process to the total equivalent strain, and to the strain path (slip pattern) change induced by shearing.

A large fraction of high angle boundaries formed in the high strain samples may result in a different annealing behavior when the samples are heated. It has been found that an equiaxed grain structure may be developed during annealing of high strain structures in a gradual or continuous manner [10, 11, 12], with small change in the fraction of high angle boundaries. The present ARB sample showed a similar annealing behavior, as seen in figure 4. The previous misorientation measurements by EBSD in the high strain samples showed that the fraction of high angle boundaries is often reaches a saturation value in a range of 65-75%. This fraction is often considered as a requirement for a continuous change in the microstructure during annealing. However, the present TEM results show that in the 6 cycle ARB processed sample, the high angle boundaries is only 56% of the total boundaries and this fraction increased to about 65% after annealing at 300°C. The higher faction of high angle boundaries obtained in the previous EBSD studies may be due to the fact that the boundaries of lower than 1-2° have been cut off by considering the angular resolution limitation of the EBSD technique [11,12]. In the present TEM study, 17.2% of the total boundaries in the as deformed ARB sample have misorientation below 2.5° (figures 1 and 2). Therefore, the fraction of the high angle boundaries in the previous studies [11,12] was overestimated. Therefore, it is concluded that there is no disagreement between the present work and the previous studies [11, 12] when relating the fraction of the high angle boundaries to the behavior of low temperature annealing. However, Figure 3 shows also the formation of some large grains, which may suggest that the annealing behavior at higher temperatures may differ from what observed in this study.

4.2 Morphology and grain size

In a previous study [5] the morphological change during annealing of similar ARB samples has been studied in more detail. It has been found that a gradual change of the initial lamellar structure into an equiaxed structure occurs when annealing at temperatures below 225°C. Such a change is complete at 225°C after annealing for 30min. During this change the structural coarsening is insignificant; the spacing measured in the normal direction (lamellar spacing) changed from 0.2 μm in the as-deformed state to 0.7 μm after the 225°C annealing. In this study, Figure 3 shows a mean (sub)grain size of about 4.5 μm and an existence of a

few relatively large grains after annealing at 300°C. This indicates an obvious grain growth during a higher temperature annealing of the equiaxed structure that is formed at 225°C. Figure 3 also shows that the bonded interfaces can be strong barriers to the grain growth. This may explain why a relatively uniform structure is formed in the ARB processed and annealed samples. However, a further study is required to examine the growth behavior at higher annealing temperatures (>300°C).

ACKNOWLEDGEMENTS

The authors gratefully acknowledge the Danish National Research Foundation for supporting the Center for Fundamental Research: Metal Structures in Four Dimensions, within which part of this work was performed and they also acknowledge the 21st century COE program, the Center of Excellence for Advanced Structural and Functional Materials Design in Osaka University, funded by the Ministry of Education, Sports, Culture, Science & Technology of Japan for the financial support. RU thanks the Uomoto international scholarship which gaves him a chance to study in Risø National Laboratory.

REFERENCES

[1] Y. Saito, N. Tsuji, H. Utsunomiya and T. Sakai: Acta Mater. **47**, 579-583 (1999).

[2] Y. Saito, N. Tsuji, H. Utsunomiya, T. Sakai and R.G. Hong: Scripta Mater. **39** 1221-1227 (1998).

[3] N.Tsuji, Y.Saito, H.Utsunomiya and S.Tanigawa: Scripta mater. vol. **40**, 795-800 (1998).

[4] N. Tsuji, Y. Ito, Y. Saito and Y. Minamino: Scripta Mater. **47**, 893-899 (2002).

[5] Y. Ito, N. Tsuji, Y. Saito, H. Utsunomiya and T. Sakai, J. Jpn. Inst. Metals **64**, 429-437 (2000).

[6] R. Ueji, X. Huang. N. Hansen, N. Tsuji and Y. Minamino, Mater. Sci. Forum, **426-432**, 405-410 (2003).

[7] Q. Liu, : J. Appl. Crystallogr. **27**, 775-781 (1994).

[8] Q. Liu, X. Huang, D.J.Lloyd and N.Hansen: Acta Mater. **50**, 3789-3802 (2002).

[9] X. Huang, N. Tsuji, N. Hansen and Y. Minamino, Mater. Sci. Eng. **A340**, 265-271 (2003).

[10] A. Scarsson, W.B. hutchinson, B. Nicol, P. S. Bate and H. E. Ekstrom, Mater. Sci. Forum, **157-162**, 1271-1276 (1994).

[11] J. R. Bowen, Ph.D. Thises, (2000), UMIST, UK.

[12] F. J. Humphreys, P. B. Prangnell, J. R. Bowen, A. Gholinia and C. Harris, Phil. Trans. R. Soc. Lond. A **357**, 1663-1681 (1999).

(Received December 1, 2003; Accepted August 19, 2004)